EP2受容体作動薬を用いた軟骨再生（口頭）	青山朋樹、戸口田淳也	第6回日本関節鏡・膝・スポーツ整形外科学会	2014.7.24-7.26	国内
我が国の一般人における2011年版Knee Society Score-ながはまコホートより一（口頭）	伊藤宣	第6回日本関節鏡・膝・スポーツ整形外科学会	2014.7.24	国内
State of Arthroplasty in Asia.（口頭）	Matsuda S	2014 ICJR Pan Pacific Congress.Kona, USA	2014.7.17	国外
Computer simulation for TKA.（口頭）	Matsuda S	2014 ICJR Pan Pacific Congress.Kona, USA	2014.7.17	国外
人工膝関節置換術～現在推奨される手術手技～.（口頭）	松田秀一	第10回島根県整形外科医会研修会	2014.7.3	国内
変形性膝関節症の保存療法.（口頭）	松田秀一	福島県県北臨床学術講演会	2014.6.25	国内
膝関節のスポーツ障害.（口頭）	松田秀一	平成26年度大分県整形外科 臨床整形外科医会	2014.6.14	国内
地域在住日本人高齢者におけるサルコペニア有症率ーAWGSアルゴリズムによる検討ー.（口頭）	山田実、西口周、青山朋樹、荒井秀典	第56回日本老年医学会学術集会	2014.6.12-6.14	国内
チラシ配布による介護予防のためのポピュレーションアプローチークラスター無作為化比較対照試験ー.（口頭）	山田実、青山朋樹、荒井秀典	第56回日本老年医学会学術集会	2014.6.12-6.14	国内
地域在住高齢者における呼吸機能と骨量との関連.（口頭）	足達大樹、西口周、山田実、青山朋樹	第56回日本老年医学会学術集会	2014.6.12-6.14	国内
膝関節痛のマネジメント.（口頭）	松田秀一	岐阜芝蘭会	2014.6.8	国内
関節軟骨基質再生のための至適温度の探究_三次元培養を用いたin vitro 研究（口頭）	伊藤明良、青山朋樹、長井桃子、太治野純一、山口将希、飯島弘貴、張項凱、秋山治彦、黒木裕士	第49 回日本理学療法学術大会	2014.5.30-6.2	国内
骨髄由来間葉系間質細胞移植治療と運動との併用は骨軟骨欠損した関節軟骨の再生を促進する.（口頭）	山口将希、青山朋樹、伊藤明良、長井桃子、太治野純一、飯島弘貴、張項凱、秋山治彦、黒木裕士	第49 回日本理学療法学術大会	2014.5.30-6.2	国内
8週間の関節不動により変性した軟骨は，不動解除後に変性が助長される（口頭）	長井桃子、青山朋樹、伊藤明良、山口将希、飯島弘貴、太治野純一、張項凱、秋山治彦、黒木裕士	第49 回日本理学療法学術大会	2014.5.30-6.2	国内
大腿骨頭壊死症に対する自己骨随由来間葉系幹細胞を用いた臨床試験におけるリハビリテーション.（口頭）	青山朋樹、藤田容子、窓場勝之、南角学、冨田素子、後藤公志、柿木良介、中村孝志、戸口田淳也	第49 回日本理学療法学術大会	2014.5.30-6.2	国内
免荷による歩容変化は再荷重によっても回復しない　後肢免荷がラットの歩容に与える影響	太治野純一、伊藤明良、張項凱、長井桃子、山口将希、飯島弘貴、青山朋樹、黒木裕士	第49 回日本理学療法学術大会	2014.5.30-6.2	国内

変形性関節症モデルラットに対する緩徐な走行運動は軟骨下骨変化を予防できるのか？（口頭）	飯島弘貴、青山朋樹、伊藤明良、長井桃子、山口将希、太治野純一、張項凱、秋山治彦、黒木裕士	第49 回日本理学療法学術大会	2014.5.30-6.2	国内
The new Knee Society Score in Japanese general population: The Nagahama Cohort Study.	Taniguchi N	The 87th Annual Meeting of the Japanese Orthopaedic Association (Kobe)	2014.5.24	国内

２．学会誌・雑誌等における論文掲載

掲載した論文（発表題目）	発表者氏名	発表した場所（学会誌・雑誌等名）	発表した時期	国内・外の別
Central blood pressure relates more strongly to retinal arteriolar narrowing than brachial blood pressure: the Nagahama Study.	Kumagai K, Tabara Y, Yamashiro K, Miyake M, Akagi-Kurashige Y, Oishi M, Yoshikawa M, Kimura Y, Tsujikawa A, Takahashi Y, Setoh K, Kawaguchi T, Terao C, Yamada R, Kosugi S, Sekine A, Nakayama T, Matsuda F, Yoshimura N; Nagahama Study group.	J Hypertens. 33:323-329.	2015年2月	国外
Regional comparisons of porcine menisci.	Zhang X, Aoyama T, Ito A, Tajino J, Nagai M, Yamaguchi S, Iijima H, Kuroki H	J Orthop Res. 32(12):1602-11.	2014年12月	国外
Association of serum-free fatty acid level with reduced reflection pressure wave magnitude and central blood pressure: the Nagahama study.	Tabara Y, Takahashi Y, Kawaguchi T, Setoh K, Terao C, Yamada R, Kosugi S, Sekine A, Nakayama T, Matsuda F; Nagahama Study Group.	Hypertension. 64:1212-1218.	2014年12月	国外
The KSS 2011 reflects symptoms, physical activities, and radiographic grades in a Japanese population.	Taniguchi N, Matsuda S, Kawaguchi T, Tabara Y, Ikezoe T, Tsuboyama T, Ichihashi N, Nakayama T, Matsuda F, Ito H	Clin Orthp Relat Res. 473(1):70-5.	2015年1月	国外
Effects of smoking and shared epitope on the production of anti-citrullinated peptide antibody in a Japanese adult population.	Terao C, Ohmura K, Ikari K, Kawaguchi T, Takahashi M, Setoh K, Nakayama T, Kosugi S, Sekine A, Tabara Y, Taniguchi A, Momohara S, Yamanaka H, Yamada R, Matsuda F, Mimori T; Nagahama Study Group.	Arthritis Care Res. 66:1818-1827.	2014年12月	国外

Association between antinuclear antibodies and the HLA class II locus and heterogeneous characteristics of staining patterns: the Nagahama study.	Terao C, Ohmura K, Yamada R, Kawaguchi T, Shimizu M, Tabara Y, Takahashi M, Setoh K, Nakayama T, Kosugi S, Sekine A, Matsuda F, Mimori T; Nagahama Study Group.	Arthritis Rheumatol. 66:3395-3403.	2014年12月	国外
Gastroesophageal reflux disease symptoms and dietary behaviors are significant correlates of short sleep duration in the general population: the Nagahama Study.	Murase K, Tabara Y, Takahashi Y, Muro S, Yamada R, Setoh K, Kawaguchi T, Kadotani H, Kosugi S, Sekine A, Nakayama T, Mishima M, Chiba T, Chin K, Matsuda F	Sleep. 37:1809-1815.	2014年11月	国外
Tooth Loss and Atherosclerosis: The Nagahama Study.	Asai K, Yamori M, Yamazaki T, Yamaguchi A, Takahashi K, Sekine A, Kosugi S, Matsuda F, Nakayama T, Bessho K; the Nagahama Study Group; the Nagahama Study Group.	J Dent Res. in press.	2014年11月	国外
Comprehensive replication of the relationship between myopia-related genes and refractive errors in a large Japanese cohort.	Yoshikawa M, Yamashiro K, Miyake M, Oishi M, Akagi-Kurashige Y, Kumagai K, Nakata I, Nakanishi H, Oishi A, Gotoh N, Yamada R, Matsuda F, Yoshimura N; Nagahama Study Group.	Invest Ophthalmol Vis Sci. 55:7343-7354.	2014年10月	国外
Three-dimensional reconstruction of rat knee joint using episcopic fluorescence image capture.	Takaishi R, Aoyama T, Zhang X, Higuchi S, Yamada S, Takakuwa T	Osteoarthritis Cartilage. 22(10):1401-9.	2014年10月	国外
Effect of physical activity on memory function in older adults with mild Alzheimer's disease and mild cognitive impairment.	Tanigawa T, Takechi H, Arai H, Yamada M, Nishiguchi S, Aoyama T	Geriatr Gerontol Int. 14(4):758-62.	2014年10月	国外
An exploratory clinical trial for idiopathic osteonecrosis of femoral head by cultured autologous multipotent mesenchymal stromal cells augmented with vascularized bone grafts.	Aoyama T, Goto K, Kakinoki R, Ikeguchi R, Ueda M, Kasai Y, Maekawa T, Tada H, Teramukai S, Nakamura T, Toguchida J	Tissue Eng Part B Rev. 20(4):233-42.	2014年8月	国外
A genome-wide association study of serum levels of prostate-specific antigen in the Japanese population.	Terao C, Terada N, Matsuo K, Kawaguchi T, Yoshimura K, Hayashi N, Shimizu M, Soga N, Takahashi M; Nagahama Cohort Study Group, Kotoura Y, Yamada R, Ogawa O, Matsuda F	J Med Genet. 51:530-536.	2014年9月	国外

Destabilization of the medial meniscus leads to subchondral bone defects and site-specific cartilage degeneration in an experimental rat model.	Iijima H, Aoyama T, Ito A, Tajino J, Nagai M, Zhang X, Yamaguchi S, Akiyama H, Kuroki H	Osteoarthritis Cartilage. 22(7):1036-43.	2014年7月	国外
Contributions of biarticular myogenic components to the limitation of the range of motion after immobilization of rat knee joint.	Nagai M, Aoyama T, Ito A, Iijima H, Yamaguchi S, Tajino J, Zhang X, Akiyama H, Kuroki H	BMC Musculoskelet Disord. 15:224.	2014年7月	国外
Quantification of changes in gait characteristics associated with intermittent claudication in patients with lumbar spinal stenosis.	Nagai K, Aoyama T, Yamada M, Izeki M, Fujibayashi S, Takemoto M, Nishiguchi S, Tsuboyama T, Neo M	J Spinal Disord Tech. 27(4):E136-42.	2014年7月	国外

４．研究成果の刊行物・別刷

Original Article

Central blood pressure relates more strongly to retinal arteriolar narrowing than brachial blood pressure: the Nagahama Study

Kyoko Kumagai[a], Yasuharu Tabara[b], Kenji Yamashiro[a], Masahiro Miyake[a], Yumiko Akagi-Kurashige[a], Maho Oishi[a], Munemitsu Yoshikawa[a], Yugo Kimura[a], Akitaka Tsujikawa[a], Yoshimitsu Takahashi[c], Kazuya Setoh[b], Takahisa Kawaguchi[b], Chikashi Terao[b], Ryo Yamada[b], Shinji Kosugi[d], Akihiro Sekine[e], Takeo Nakayama[c], Fumihiko Matsuda[b], Nagahisa Yoshimura[a], on behalf of the Nagahama Study group

Objectives: Although central blood pressure (BP) is considered to be more closely associated with large arterial remodeling and cardiovascular outcomes than brachial BP, few studies have investigated these associations with changes in small arteries. As morphological changes in retinal vessels might be associated with cardiovascular outcomes, we conducted a cross-sectional study to investigate the association of central BP with retinal vessel caliber.

Methods: The study included 8054 Japanese participants. Central BP was estimated by the radial arterial waveform by calibrating brachial BP. Central retinal arteriolar equivalent (CRAE) was computationally measured using fundus photography.

Results: CRAE was most strongly associated with central SBP ($r=-0.324$, $P<0.001$), followed by DBP ($r=-0.292$, $P<0.001$) and central pulse pressure (PP; $r=-0.226$, $P<0.001$). The correlation coefficient between SBP and CRAE was significantly greater in central SBP than in brachial SBP ($r=-0.300$, $P<0.001$). After adjustment for possible covariates, brachial SBP ($\beta=-0.221$, $P<0.001$) and central SBP ($\beta=-0.239$, $P<0.001$) were independently associated with CRAE. Further, higher brachial SBP ($\beta=-0.226$, $P<0.001$) and smaller PP amplification ($\beta=0.092$, $P<0.001$) were identified as independent determinants of narrowing of CRAE in the same equation, which indicated the superiority of central BP. Central BP-determined hypertensive individuals had a significantly narrower CRAE independent of brachial BP (central/brachial: hypertension/hypertension 121.4 ± 11.5, hypertension/normotension 120.9 ± 11.2, normotension/hypertension 125.1 ± 11.9, normotension/normotension 128.1 ± 11.5 μm).

Conclusion: Central BP was more closely associated with the narrowing of CRAE than brachial BP. Slight increases in central BP might be involved in the morphological changes in small retinal arteries, even in individuals with optimal brachial BP.

Keywords: central blood pressure, retinal vessel caliber, small artery narrowing

Abbreviations: AIx, augmentation index; BP, blood pressure; baPWV, brachial-to-ankle pulse-wave velocity; CRAE, central retinal arteriolar equivalent; CRVE, central retinal venular equivalent; MRRM, Meng–Rosenthal–Rubin method; SBP2, late SBP

INTRODUCTION

Central aortic blood pressure (BP) directly reflects the BP load on target organs and is therefore considered to be more closely associated with the cardiovascular outcomes than brachial BP. Compared with brachial BP, central BP estimated via radial arterial waveform or measured via carotid tonometry is more effective in showing the degree of association with intima–media thickness of the carotid artery in hypertensive individuals [1], the severity of coronary stenosis in patients with coronary artery diseases [2], the incidence of cardiovascular disease in the general population [3], and all-cause mortality in patients with end-stage renal disease [4]. One reason for these discrepancies is the difference in pulse pressure (PP) between the brachial artery and central aorta (PP amplification), which is largely dependent on the velocity of the reflection pressure wave. Increased pulse-wave velocity

Journal of Hypertension 2015, 33:323–329

[a]Department of Ophthalmology and Visual Sciences, [b]Center for Genomic Medicine, Kyoto University Graduate School of Medicine, [c]Department of Health Informatics, [d]Department of Medical Ethics and Medical Genetics, Kyoto University School of Public Health and [e]Kyoto University Medical Research Support Center, Kyoto, Japan

Correspondence to Yasuharu Tabara, Center for Genomic Medicine, Kyoto University Graduate School of Medicine, Shogoin-kawaramachi, Sakyo-ku, Kyoto, 606-8507, Japan. Tel: +81 75 366 7407; fax: +81 75 751 4167; e-mail: tabara@genome.med.kyoto-u.ac.jp

Received 15 March 2014 **Revised** 20 August 2014 **Accepted** 20 August 2014

J Hypertens 33:323–329

DOI:10.1097/HJH.0000000000000391

(PWV) augments overlapping of the reflection pressure wave on the forward pressure wave, which strengthens the forward wave and in turn increases central aortic BP.

High BP load is also a causative factor for small-vessel diseases such as silent cerebral infarction [5]. Retinal vessels are the only visible arterioles and venules whose caliber can be easily measured by fundus photography. Retinal vessel signs, that is, the narrowing of retinal arteriolar caliber and widening of venular caliber, have been associated with cardiovascular risk factors [6,7], systemic inflammation [8], and decreased renal function [9]. Further, because of the similar anatomic features and physiological properties of retinal vessels and cerebral microvessels [10], retinal vessel caliber has been suggested to predict stroke incidence [11,12] and stroke death [13]. Recently, Ott *et al.* [14] assessed the retinal arteriolar wall-to-lumen ratio in 135 nondiabetic individuals and reported that central PP was significantly associated with retinal arteriolar remodeling, though the superiority of central BP to brachial BP was not evaluated. Muiesan *et al.* [15] also reported a significant correlation between central BP and media-to-lumen ratio of subcutaneous small resistance arteries, but again did not evaluate the superiority of central BP. Although it remains unclear whether changes in retinal vessel caliber represent structural changes in small arteries and arterioles, a strong correlation between arterial diameter and medial cross-sectional area has been observed in the subcutaneous small arteries [16]. Further, by considering a substantial number of studies that reported a clinical and prognostic significance of retinal vascular caliber measurements [17], it is promising that retinal vascular calibers represent the vascular disease risks in various kinds of populations. Given these backgrounds, it was speculated that central BP might also be more closely correlated with the pathophysiological changes in retinal vessel calibers than brachial BP, whereas a paradoxical result was reported [18].

Here, we conducted a large-scale cross-sectional study in a general population to clarify the possibility of a superior association of central BP with not only large arterial diseases, but also small-vessel properties by measuring retinal arteriolar and venular calibers. Given that the prognostic significance of retinal vessel properties on the cardiovascular and cerebrovascular outcomes has been suggested, our results might be of clinical and epidemiological significance to the possible addition of central BP measurement to conventional brachial measurement in the assessment of small arterial disease risks.

METHODS

Study participants

Participants consisted of 8054 apparently healthy middle-aged to elderly citizens who were participants of the Nagahama Prospective Cohort for Comprehensive Human Bioscience (the Nagahama Study). The Nagahama Study cohort was recruited from 2008 to 2010 from the general population living in Nagahama City, a largely suburban city of 125 000 inhabitants located in central Japan. Community residents aged 30–74 years, living independently in the community and with no physical impairment or dysfunction, were recruited for the Nagahama cohort. Of a total of 9804 participants, those meeting any of the following conditions were excluded from this study, which are as follows: unsuccessful measurement of retinal vascular caliber ($n=1521$), presence of retinal vein occlusion or collateral vessels in either eye ($n=78$), unsuccessful assessment of retinopathy ($n=45$) or clinical parameters required for this study ($n=57$), extreme deviation of renal function [estimated glomerular filtration rate $194 \times \text{creatinine}^{-1.094} \times \text{age}^{-0.287} \times 0.739$ (if women)] less than 30 ml/min per m^2 ($n=7$), and women who were pregnant ($n=42$). All study procedures were approved by the ethics committee of Kyoto University Graduate School of Medicine and the Nagahama Municipal Review Board. Written informed consent was obtained from all the participants.

Blood pressure measurements

Radial arterial waveform and brachial BP were measured simultaneously (HEM-9000AI; Omron Healthcare, Kyoto, Japan) after 5 min rest in the sitting position. Measurements were taken twice, and the mean value was used in the analysis. Absolute pressure of the late systolic peak (SBP2) of the radial arterial waveform was considered the central SBP. The radial augmentation index (AIx) was calculated from the waveform as the ratio of the late systolic peak to the first systolic peak, and the BP measurements are briefly described in the Supplemental Methods. PP amplification was calculated by subtracting central PP from brachial PP and expressed in the absolute values (mmHg). Mean BP (MBP) was calculated from SBP and DBP using the following formula: $(\text{SBP}-\text{DBP})/3+\text{DBP}$. Hypertension was defined as any or all of the following: use of antihypertensive medication, DBP greater than 90 mmHg, or brachial SBP greater than 140 mmHg or central SBP greater than 130 mmHg according to a previous report [19] that estimated central BP using the SphygmoCor system. SBP2 measured by the HEM-9000AI was almost identical to central SBP measured by the SphygmoCor system [20].

Retinal vessel caliber measurements

Fundus photographs of both eyes were taken in a shaded area using a 45-degree digital nonmydriatic camera (CR-DG10; Canon, Tokyo, Japan) at a 5-degree angle from the nasal side of the macula. A fundus photograph of the right eye was used for retinal caliber measurements. Retinal vascular caliber was measured using a semi-automated computer-based program (IVAN; University of Wisconsin, Madison, Wisconsin, USA). The measurement of central retinal arteriolar equivalent (CRAE) and central retinal venular equivalent (CRVE) are briefly described in the Supplemental Methods. Intragrader and intergrader intraclass correlation coefficients for the retinal arteriolar measurements were 0.80 ± 0.06 and 0.75 ± 0.06, and for the venular caliber measurements were 0.88 ± 0.13 and 0.86 ± 0.01, respectively.

Assessment of retinopathy

Retinopathy of both eyes was independently assessed in a masked fashion by two ophthalmologists, with a third

ophthalmologist making a final decision in cases of disagreement. Retinopathy was defined by the Early Treatment Diabetic Retinopathy Study Severity Scale [21] by the presence of any of the following characteristic lesions: microaneurysms, retinal hemorrhages, cotton wool spots, hard exudates, intraretinal microvascular abnormalities, venous beading, vitreous hemorrhages, or neovascularization. Individuals having at least one characteristic lesion in either eye were diagnosed as having retinopathy.

Basic clinical parameters

Basic clinical parameters, including plasma markers, were measured at baseline. Age was calculated from the year of birth to the year of baseline measurements. Smoking, alcohol consumption, and a history of cardiovascular disease, namely symptomatic stroke or ischemic heart disease, were determined using a structured self-administered questionnaire. Daily alcohol consumption was determined using the standard Japanese alcohol unit (1 unit corresponds to 22.9 g of ethanol). Brachial-to-ankle pulse-wave velocity (baPWV) was measured as an index of arterial stiffness. The method of baPWV measurement is detailed in the Supplemental Methods. Collinearity of baPWV with a carotid-to-femoral PWV, a standard measure of arterial stiffness, has been reported elsewhere [22].

Statistical analysis

Comparison of overlapping correlation coefficients was performed using the Meng–Rosenthal–Rubin method (MRRM). Identification of the factors independently associated with retinal vessel caliber, and the assessment of differences in CRAE by hypertension status was performed using multiple regression analysis. Statistical analysis was performed using JMP 9.0.2 software (SAS Institute, Cary, North Carolina, USA) and R software. A P value of less than 0.05 was considered to indicate statistical significance.

RESULTS

Clinical characteristics of the study participants are shown in Table 1. Mean age was 52 ± 13 years old. There were approximately two times more female than male participants. We excluded 1750 individuals from the analysis, mostly because of the unsuccessful measurement of retinal vessel caliber. Although the excluded participants were significantly older (Figure S1), BP levels of these excluded individuals and roughly measured retinal vessel calibers in a part of the individuals ($n = 229$) were not different from those of the remaining study participants (Table S1, http://links.lww.com/HJH/A416).

Distribution of CRAE and CRVE is shown in Figure S2, http://links.lww.com/HJH/A416. There was a moderate interrelationship between CRAE and CRVE ($r = 0.352$, $P < 0.001$). CRVE was significantly larger in men than in women (183.8 ± 15.9 vs. 178.7 ± 15.1 μm, $P < 0.001$). In contrast, CRAE was only slightly different between men and women (125.7 ± 12.0 vs. 126.3 ± 11.8 μm, $P = 0.016$). Basic factors that were significantly associated with retinal vessel caliber included age (CRAE, $r = -0.210$, $P < 0.001$; CRVE, $r = -0.204$, $P < 0.001$), habitual smoking (CRAE: current smoker 128.7 ± 11.7 μm, nonsmoker 125.7 ± 11.9 μm, $P < 0.001$; CRVE: 187.3 ± 15.8, 179.2 ± 15.1 μm, $P < 0.001$), and drinking (CRAE: habitual drinker 125.2 ± 11.9 μm, nondrinker 126.6 ± 11.9 μm, $P < 0.001$; CRVE: 182.0 ± 15.8, 179.6 ± 15.3 μm, $P < 0.001$). Figure 1 shows the age-related changes in BP, baPWV, and retinal vessel caliber. Changes in CRAE and CRVE were symmetrical to those in MBP, and were predominant in middle age, whereas the progression of large arterial stiffness evaluated by baPWV was greater in older age.

TABLE 1. Participants characteristics ($n = 8054$)

Age (years old)	52 ± 13
Sex (male, %)	32.5
Body height (cm)	160.4 ± 8.4
Body weight (kg)	57.4 ± 11.0
BMI (kg/m^2)	22.2 ± 3.3
Waist circumference (cm)	80.0 ± 9.2
Smoking (current/past/never, %)	15.1/20.1/64.8
Alcohol drinking (habitual/occasional/never, %)	22.4/10.4/67.2
Daily alcohol consumption (Japanese alcohol unit)	0.60 ± 0.99
History of cardiovascular disease (%)	2.3
Brachial SBP (mmHg)	122 ± 17
Central SBP (mmHg)	113 ± 18
Brachial PP (mmHg)	47 ± 11
Central PP (mmHg)	37 ± 11
PP amplification (mmHg)	10 ± 6
DBP (mmHg)	76 ± 11
Radial AIx (%)	80 ± 14
Heart rate (beats/min)	69 ± 10
Antihypertensive medication (%)	14.6
baPWV (cm/s)	1245 ± 218
CRAE (μm)	126.1 ± 11.9
CRVE (μm)	180.4 ± 15.5
Retinopathy (%)	5.8
Axial length (mm)	24.0 ± 1.3

Values are mean ± standard deviation. Cardiovascular disease includes symptomatic stroke or ischemic heart disease. AIx, augmentation index; baPWV, brachial-to-ankle pulse-wave velocity; CRAE, central retinal arteriolar equivalent; CRVE, central retinal venular equivalent; PP, pulse pressure.

The correlations of BP with CRAE and CRVE are summarized in Table 2. CRAE was strongly associated with SBP, followed by DBP, PP, radial AIx, and PP amplification. Results of MRRM analysis indicated that the correlation coefficient between BPs and CRAE was significantly larger in central BP than brachial BP even after applying the Bonferroni correction ($P = 0.05/16 = 0.003$). Approximately 6% of individuals were diagnosed with retinopathy (Table 1). These individuals were significantly older, and had higher brachial and central SBP (Table S2, http://links.lww.com/HJH/A416). However, the results of a sensitivity analysis (Table S3, http://links.lww.com/HJH/A416) indicated that the superiority of central BP in association with CRAE was independent of retinopathy (model B), as well as of antihypertensive treatment (model C), history of cardiovascular diseases (model D), and metabolic syndrome (model E).

Table 3 shows the results of multiple linear regression analysis for CRAE. After adjustment for possible covariates, brachial SBP (model 1) and central SBP (model 2) were independently associated with CRAE. Further, in the equation that included both brachial SBP and PP amplification, higher brachial SBP and smaller PP amplification were independently associated with the narrowing of CRAE

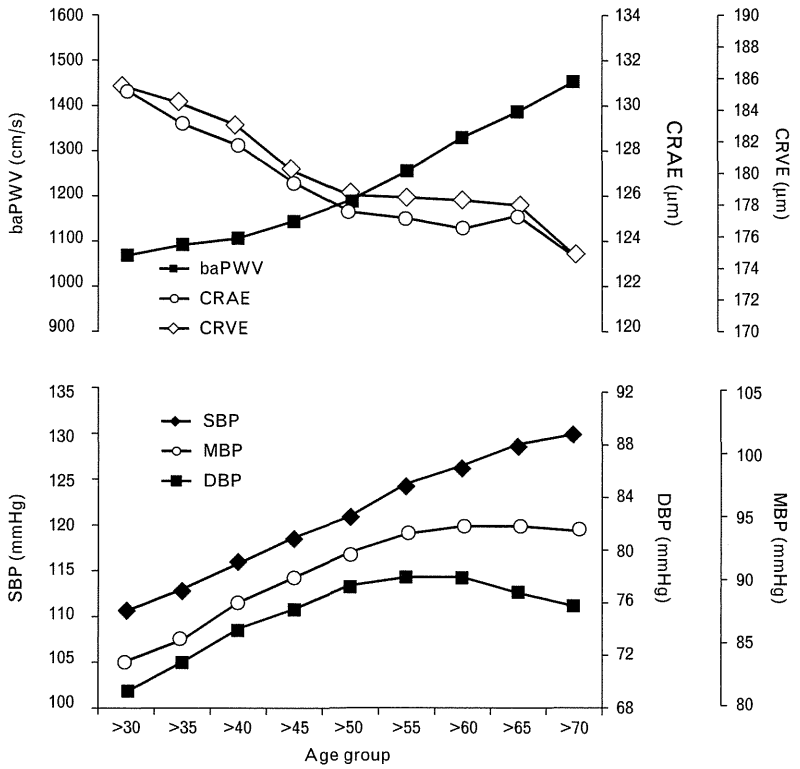

FIGURE 1 Age-related changes in retinal vessel calibers and arterial parameters. Each symbol represents the mean of individuals not taking antihypertensive drugs ($n = 6877$). baPWV, brachial-to-ankle pulse-wave velocity; CRAE, central retinal arteriolar equivalent; CRVE, central retinal venular equivalent.

(model 3), suggesting that a relatively high central PP is a risk for the narrowing of CRAE. Radial AIx was significantly associated with CRAE in a model that included brachial SBP (model 4), but not central SBP (model 5). In contrast, central SBP was not an important determinant for CRVE (central SBP, $\beta = -0.031$, $P = 0.026$).

Multiple linear regression analysis for retinal vessel caliber (Table 4) indicated that CRAE was strongly associated with BP. In contrast, CRVE was affected by various factors, namely body fluid parameters including hematocrit and white blood cell count, body weight, and smoking, and had only a weak association with MBP. Metabolic and hematological characteristics of the study participants are summarized in Tables S4 and S5, http://links.lww.com/HJH/A416.

Figure 2a shows the differences in mean CRAE by hypertension status defined by central and brachial BP. Central BP-determined hypertensive individuals had a significantly narrower CRAE that was independent of brachial BP. Further, CRAE was linearly decreased with increasing central BP even within the same brachial BP levels (Fig. 2b). By a simple correlation analysis, central SBP corresponded to an approximately 10 mmHg lower brachial SBP (central SBP $= -7.15 + 0.98 \times$ brachial SBP). Individuals exhibiting a relatively lower central SBP, that is, whose central SBP was more than 10 mmHg lower than brachial SBP, had a wider CRAE than those whose central SBP was at a similar level to brachial SBP. In contrast, individuals exhibiting a relatively higher central SBP showed a narrower CRAE.

TABLE 2. Correlation between BP and retinal vessel caliber

	CRAE				CRVE			
	Simple correlation		MRRM		Simple correlation		MRRM	
	r	*P*	*z*	*P*	*r*	*P*	*z*	*P*
Brachial SBP (mmHg)	−0.300	<0.001	6.85	<0.001	−0.107	<0.001	11.65	<0.001
Central SBP (mmHg)	−0.324	<0.001			−0.149	<0.001		
Brachial PP (mmHg)	−0.181	<0.001	7.87	<0.001	−0.108	<0.001	11.65	<0.001
Central PP (mmHg)	−0.226	<0.001			−0.176	<0.001		
DBP (mmHg)	−0.292	<0.001			−0.064	<0.001		
Radial AIx (%)	−0.163	<0.001			−0.175	<0.001		
PP amplification (mmHg)	−0.105	<0.001			0.142	<0.001		

Overlapping correlation coefficients were compared with the Meng–Rosenthal–Rubin method (MRRM). AIx, augmentation index; CRAE, central retinal arteriolar equivalent; CRVE, central retinal venular equivalent; PP, pulse pressure.

TABLE 3. Multiple linear regression analysis for CRAE

	Model 1		Model 2		Model 3		Model 4		Model 5	
	β (VIF)	P	β (VIF)	P	β (VIF)	P	β (VIF)	P	β (VIF)	P
Brachial SBP (mmHg)	−0.221 (1.90)	<0.001			−0.226 (1.91)	<0.001	−0.206 (1.98)	<0.001		
Central SBP (mmHg)			−0.239 (1.84)	<0.001					−0.244 (2.46)	<0.001
PP amplification (mmHg)					0.092 (1.50)	<0.001				
AIx (%)							−0.072 (1.86)	<0.001	0.009 (2.40)	0.545

Adjusted factors were as follows: age, sex, body height, body weight, current smoking, daily alcohol consumption, history of cardiovascular diseases, antihypertensive medication, heart rate, brachial-to-ankle pulse-wave velocity, axial length, retinopathy, and fellow retinal vessel caliber. β, standardized regression coefficient; AIx, augmentation index; CRAE, central retinal arteriolar equivalent; PP, pulse pressure; VIF, variance inflation factor.

DISCUSSION

In this study of an apparently healthy general population, we observed that central BP was more closely associated with the narrowing of CRAE than brachial BP. Even in individuals diagnosed as normotensive by brachial BP, slight increases in central SBP might be a risk factor for the narrowing of CRAE.

We clarified the stronger association of central SBP with the morphological changes in small arterioles, though close associations between central BPs and pathophysiological changes in large arteries [1,2] and cardiovascular morbidity [3] have already been demonstrated. In contrast, central SBP was not a major determinant for venular caliber. Given the strong correlation between BPs and CRAE but not CRVE, changes in arteriolar caliber might more accurately reflect the pressure load of the central aorta. Previous cross-sectional population-based studies have suggested that the associations of retinal vessel caliber with the cardiovascular risk factors largely differs between CRAE and CRVE, with most observing a strong association between brachial BP and the narrowing of CRAE rather than the widening of CRVE [6,7,23,24]. The wide range of covariates for CRVE (Table 4) might also be a reason for the weak association between BPs and CRVE.

Correlation coefficient between central SBP and CRAE was stronger than that of the brachial SBP (Table 2). As a result of the strong collinearity between brachial and central SBP, we could not directly compare the superiority by including both SBPs in a same regression model. However, in the model that included brachial SBP and PP amplification (Table 3, model 3), both the parameters were identified as independent determinant for CRAE. As central SBP is a function of brachial SBP and PP amplification, the results indirectly support the superiority of central SBP in association with CRAE. Further, radial AIx was independently associated with CRAE in a model that included brachial SBP (Table 3, model 4). However, when central SBP was exchanged for brachial SBP (model 5), the association between AIx and CRAE became insignificant. These results suggest that the absolute value of central aortic pressure rather than the ratio of forward and reflection pressure waves may be important for retinal arteriolar narrowing.

A recent longitudinal study of cardiovascular mortality [19] reported that a central BP of 130/90 mmHg has the best discriminatory power in the prediction of cardiovascular outcomes. In addition, a cross-sectional study based on 10 756 Japanese participants reported a central SBP of 129 mmHg as a reference value of normal BP [25]. Here, we found a significantly narrower CRAE in individuals whose central SBP exceeded 130 mmHg independent of the brachial BP levels. Further, the narrowing of CRAE was observed in cases with even lower central SBP. Small arteries may be adversely impacted by even minor increases in central BP load, even in those within the normal limits.

Results from the Strong Heart Study of Native Americans showed that PP measured at the central aorta or brachial artery was more strongly associated than SBP at any artery with large arterial remodeling, namely increased carotid intima–media thickness, vascular mass, and plaque score

TABLE 4. Multiple linear regression analysis for retinal vessel caliber

	CRAE		CRVE	
	β	P	β	P
Body height (cm)	0.079	<0.001	−0.023	0.184
Body weight (kg)	−0.017	0.255	0.136	<0.001
Currently smoking	0.048	<0.001	0.068	<0.001
Hyperglycemia	0.012	0.226	−0.017	0.106
Dyslipidemia	0.010	0.360	0.018	0.103
White blood cell count (×10²/μl)	−0.008	0.436	0.073	<0.001
Hematocrit (%)	−0.042	0.001	0.115	<0.001
Mean BP (mmHg)	−0.249	<0.001	−0.056	<0.001
baPWV (cm/s)	−0.017	0.259	−0.008	0.596

Metabolic and hematological characteristics of patients are shown in Tables S4 and S5, http://links.lww.com/HJH/A416, respectively. Hyperglycemia was defined as either or both of plasma glucose greater than 126 mg/dl (fasting) or 200 mg/dl (nonfasting), or the use of hypoglycemic treatment, including insulin therapy. Individuals who met any of the following criteria were diagnosed with dyslipidemia: LDL-cholesterol greater than 140 mg/dl, HDL-cholesterol lower than 40 mg/dl, triglyceride greater than 150 mg/dl, or the use of lipid-lowering drugs. Adjustment factors were as follows: age, sex, daily alcohol consumption, history of cardiovascular disease, antihypertensive medication, heart rate, axial length, retinopathy, fellow retinal vessel caliber, and fasting time. β, standardized regression coefficient; baPWV, brachial-to-ankle pulse-wave velocity; CRAE, central retinal arteriolar equivalent; CRVE, central retinal venular equivalent.

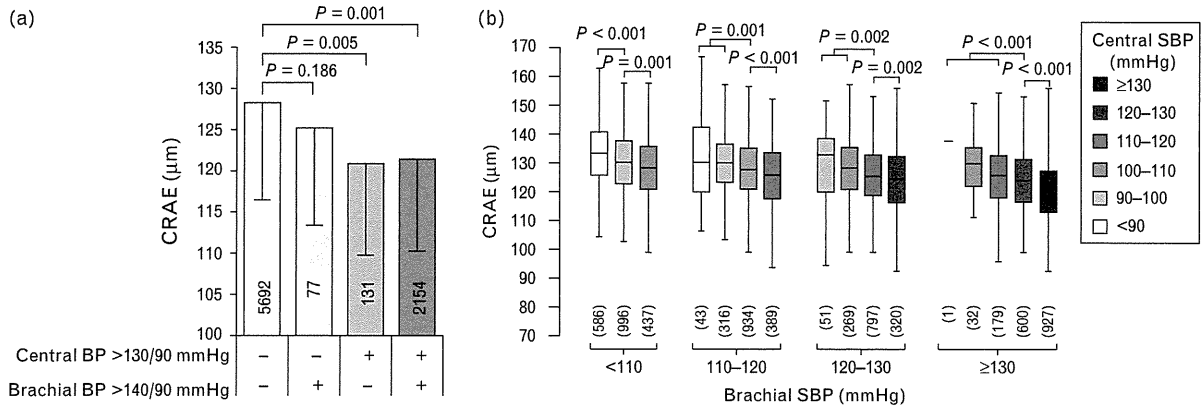

FIGURE 2 Differences in mean CRAE by central and brachial BP levels. (a) Values are mean ± standard deviation. Participants were classified into four groups according to the hypertension status as defined by central BP (any or all of central SBP ≥130 mmHg, DBP ≥90 mmHg, or use of antihypertensive medications) or brachial BP (any or all of brachial SBP ≥140 mmHg, DBP ≥90 mmHg, or use of antihypertensive medications). (b) Box plot of mean CRAE in patients not prescribed antihypertensive drugs ($n = 6877$) by various brachial and central BP levels. Statistical significance was assessed by a multiple linear regression analysis adjusted for age, sex, body height, body weight, current smoking, daily alcohol consumption, history of cardiovascular diseases, heart rate, brachial-to-ankle pulse-wave velocity, axial length, retinopathy, and CRVE. The number of patients in each subgroup is shown in the figure. CRAE, central retinal arteriolar equivalent; CRVE, central retinal venular equivalent.

[3]. The superiority of PP in prognosis for all-cause mortality was also reported from a longitudinal study based on patients with end-stage renal disease [4]. In contrast, we observed a close association between CRAE and SBPs rather than PPs. Remodeling of large arteries decreases the Windkessel function of the aorta, which increases the SBP, decreases DBP, and consequently increases PP. In contrast, systemic remodeling of small arteries increases both SBP and DBP. The different pathophysiological features of large and small arterial remodeling in association with BPs might be a factor that explains the stronger association of SBP with the narrowing of CRAEs.

Several limitations of our study warrant mention. First, we estimated central SBP using radial arterial waveform analysis, that is, late systolic peak of the radial arterial waveform (SBP2) was considered equivalent to central SBP. SBP2 was recently reported to not always represent central SBP accurately, particularly in cases with a type C aortic pressure waveform, in which peak SBP precedes an inflection point [26]. The type C waveform is observed in young individuals [27]. Therefore, misestimation of central SBP, if any, might have had no substantial impact on the present findings which were obtained from individuals aged 30 years or older. Second, we excluded a considerable number of potential individuals from analysis, mostly because of the unsuccessful measurement of retinal vessel caliber as a result of an increased frequency of cataracts, small pupils, and difficulties with ocular fixation. However, our ungradable rate 15.5% (1521 of 9804) was not too high compared with that of other large-scale epidemiological studies using the same semi-automated computer system to measure retinal vascular calibers: Atherosclerosis Risk In Communities study, 19% [28]; Beaver Dam Eye Study, 13.8% [29]; and Rotterdam study, 16.3% [30]. Further, as BP level and retinal vessel caliber of the excluded individuals did not differ from those of the included participants, the findings are unlikely confounded by the selection bias. Third, as this study was a cross-sectional setting, further longitudinal studies are needed to clarify the prognostic significance of central hemodynamics in retinal vessel morphological change.

In summary, we have clarified for the first time that central BP is strongly associated with the narrowing of retinal arteriolar caliber in a large-scale general population. As narrowing of the retinal artery is suggested to represent a subclinical cardiovascular and cerebrovascular risk and has been associated with poor prognosis, our study supports the importance of evaluating central BP in the assessment of small arterial disease risks.

ACKNOWLEDGEMENTS

The authors thank Dr Yoshihiko Kotoura, Dr Miyaki Koichi, and Dr Ishizaki Tatsuro for their help regarding clinical measurements, Nagahama City Office, and the Zeoji Club, a non-profit organization, for their assistance in conducting this study. The authors thank the editors of DMC Corporation for their help in the preparation of this manuscript.

Financial support: This study was supported by a University Grant, and a Grant-in-Aid for Scientific Research from the Ministry of Education, Culture, Sports, Science & Technology in Japan, and a research grant from the Takeda Science Foundation.

Conflicts of interest

The authors have no conflicts of interest to disclose.

REFERENCES

1. Boutouyrie P, Bussy C, Lacolley P, Girerd X, Laloux B, Laurent S. Association between local pulse pressure, mean blood pressure, and large-artery remodeling. *Circulation* 1999; 100:1387–1393.
2. Waddell TK, Dart AM, Medley TL, Cameron JD, Kingwell BA. Carotid pressure is a better predictor of coronary artery disease severity than brachial pressure. *Hypertension* 2001; 38:927–931.
3. Roman MJ, Devereux RB, Kizer JR, Lee ET, Galloway JM, Ali T, *et al.* Central pressure more strongly relates to vascular disease and outcome than does brachial pressure: the Strong Heart Study. *Hypertension* 2007; 50:197–203.
4. Safar ME, Blacher J, Pannier B, Guerin AP, Marchais SJ, Guyonvarc'h PM, London GM. Central pulse pressure and mortality in end-stage renal disease. *Hypertension* 2002; 39:735–738.
5. Pantoni L. Cerebral small vessel disease: from pathogenesis and clinical characteristics to therapeutic challenges. *Lancet Neurol* 2010; 9:689–701.

6. Liew G, Sharrett AR, Wang JJ, Klein R, Klein BE, Mitchell P, Wong TY. Relative importance of systemic determinants of retinal arteriolar and venular caliber: the atherosclerosis risk in communities study. *Arch Ophthalmol* 2008; 126:1404–1410.
7. Wong TY, Islam FM, Klein R, Klein BE, Cotch MF, Castro C, *et al.* Retinal vascular caliber, cardiovascular risk factors, and inflammation: the multiethnic study of atherosclerosis (MESA). *Invest Ophthalmol Vis Sci* 2006; 47:2341–2350.
8. De Jong FJ, Ikram MK, Witteman JC, Hofman A, de Jong PT, Breteler MM. Retinal vessel diameters and the role of inflammation in cerebrovascular disease. *Ann Neurol* 2007; 61:491–495.
9. Sabanayagam C, Shankar A, Koh D, Chia KS, Saw SM, Lim SC, *et al.* Retinal microvascular caliber and chronic kidney disease in an Asian population. *Am J Epidemiol* 2009; 169:625–632.
10. Wong TY. Is retinal photography useful in the measurement of stroke risk? *Lancet Neurol* 2004; 3:179–183.
11. McGeechan K, Liew G, Macaskill P, Irwig L, Klein R, Klein BE, *et al.* Prediction of incident stroke events based on retinal vessel caliber: a systematic review and individual-participant meta-analysis. *Am J Epidemiol* 2009; 170:1323–1332.
12. Doubal FN, Hokke PE, Wardlaw JM. Retinal microvascular abnormalities and stroke: a systematic review. *J Neurol Neurosurg Psychiatry* 2009; 80:158–165.
13. Wang JJ, Liew G, Klein R, Rochtchina E, Knudtson MD, Klein BE, *et al.* Retinal vessel diameter and cardiovascular mortality: pooled data analysis from two older populations. *Eur Heart J* 2007; 28:1984–1992.
14. Ott C, Raff U, Harazny JM, Michelson G, Schmieder RE. Central pulse pressure is an independent determinant of vascular remodeling in the retinal circulation. *Hypertension* 2013; 61:1340–1345.
15. Muiesan ML, Salvetti M, Rizzoni D, Paini A, Agabiti-Rosei C, Aggiusti C, *et al.* Pulsatile hemodynamics and microcirculation: evidence for a close relationship in hypertensive patients. *Hypertension* 2013; 61:130–136.
16. Izzard AS, Rizzoni D, Agabiti-Rosei E, Heagerty AM. Small artery structure andhypertension: adaptive changes and target organ damage. *J Hypertens* 2005; 23:247–250.
17. Ikram MK, Ong YT, Cheung CY, Wong TY. Retinal vascular caliber measurements: clinical significance, current knowledge and future perspectives. *Ophthalmologica* 2013; 229:125–136.
18. Salvetti M, AgabitiRosei C, Paini A, Aggiusti C, Cancarini A, Duse S, *et al.* Relationship of wall-to-lumen ratio of retinal arterioles with clinic and 24-h blood pressure. *Hypertension* 2014; 63:1110–1115.
19. Cheng HM, Chuang SY, Sung SH, Yu WC, Pearson A, Lakatta EG, *et al.* Derivation and validation of diagnostic thresholds for central blood pressure measurements based on long-term cardiovascular risks. *J Am Coll Cardiol* 2013; 62:1780–1787.
20. Hirata K, Kojima I, Momomura S. Noninvasive estimation of central blood pressure and the augmentation index in the seated position: a validation study of two commercially available methods. *J Hypertens* 2013; 31:508–515.
21. Grading diabetic retinopathy from stereoscopic color fundus photographs – an extension of the modified Airlie House classification. ETDRS report number 10. Early Treatment Diabetic Retinopathy Study Research Group. *Ophthalmology* 1991; 98:786–806.
22. Tanaka H, Munakata M, Kawano Y, Ohishi M, Shoji T, Sugawara J, *et al.* Comparison between carotid–femoral and brachial–ankle pulse wave velocity as measures of arterial stiffness. *J Hypertens* 2009; 27:2022–2027.
23. Sun C, Liew G, Wang JJ, Mitchell P, Saw SM, Aung T, *et al.* Retinal vascular caliber, blood pressure, and cardiovascular risk factors in an Asian population: the Singapore Malay Eye Study. *Invest Ophthalmol Vis Sci* 2008; 49:1784–1790.
24. Ikram MK, de Jong FJ, Vingerling JR, Witteman JC, Hofman A, Breteler MM, de Jong PT. Are retinal arteriolar or venular diameters associated with markers for cardiovascular disorders? The Rotterdam Study. *Invest Ophthalmol Vis Sci* 2004; 45:2129–2134.
25. Takase H, Dohi Y, Kimura G. Distribution of central blood pressure values estimated by Omron HEM-9000AI in the Japanese general population. *Hypertens Res* 2013; 36:50–57.
26. Lin MM, Cheng HM, Sung SH, Liao CF, Chen YH, Huang PH, Chen CH. Estimation of central aortic systolic pressure from the second systolic peak of the peripheral upper limb pulse depends on central aortic pressure waveform morphology. *J Hypertens* 2012; 30:581–586.
27. Murgo JP, Westerhof N, Giolma JP, Altobelli SA. Aortic input impedance in normal man: relationship to pressure wave forms. *Circulation* 1980; 62:105–116.
28. Hubbard LD, Brothers RJ, King WN, Clegg LX, Klein R, Cooper LS, *et al.* Methods for evaluation of retinal microvascular abnormalities associated with hypertension/sclerosis in the Atherosclerosis Risk in Communities Study. *Ophthalmology* 1999; 106:2269–2280.
29. Wong TY, Klein R, Klein BE, Meuer SM, Hubbard LD. Retinal vessel diameters and their associations with age and blood pressure. *Invest Ophthalmol Vis Sci* 2003; 44:4644–4650.
30. Ikram MK, Janssen JA, Roos AM, Rietveld I, Witteman JC, Breteler MM, *et al.* Retinal vessel diameters and risk of impaired fasting glucose or diabetes: the Rotterdam study. *Diabetes* 2006; 55:506–510.

Reviewers' Summary Evaluations

Reviewer 2

In a cross-sectional analysis of over 8000 middle-aged to older Japanese adults, the authors report that central SBP as measured by radial artery waveform is more strongly related to retinal arteriolar narrowing than brachial artery SBP. The cohort size is impressive and the findings are seemingly novel in relating retinal arteriolar narrowing to central pressures as opposed to brachial pressures, as has been in prior studies. Study limitations include its observational design and exclusion of large number of enrolled subjects (>1500) because of having been unable to successfully measure retinal arteriolar diameter.

Reviewer 3

In this large cohort study central blood pressure has been found to be associated with retinal arteriolar narrowing independently of brachial blood pressure. The paper focuses the attention on a topic of marked interest employing an outstanding methodology.

Regional Comparisons of Porcine Menisci

Xiangkai Zhang,[1] Tomoki Aoyama,[2] Akira Ito,[1] Junichi Tajino,[1] Momoko Nagai,[1] Shoki Yamaguchi,[1] Hirotaka Iijima,[1] Hiroshi Kuroki[1]

[1]Department of Motor Function Analysis, Human Health Sciences, Graduate School of Medicine, Kyoto University, Kyoto, Japan, [2]Department of Development and Rehabilitation of Motor Function, Human Health Sciences, Graduate School of Medicine, Kyoto University, Kyoto, Japan

Received 6 February 2014; accepted 10 June 2014
Published online 7 September 2014 in Wiley Online Library (wileyonlinelibrary.com). DOI 10.1002/jor.22687

ABSTRACT: The purpose of this study was to analyze histologic, biochemical, and biomechanical differences between zonal, regional, and anatomic locations of porcine menisci. We evaluated six menisci removed from pigs. Medial and lateral menisci were divided into three regions: anterior, middle, and posterior. In each portion, the central zone (CZ) and peripheral zone (PZ) were examined histologically (hematoxylin & eosin, safranin O/Fast green, and picrosiriusred staining), using scanning electron microscopy, biochemically (hydroxyproline assay for collagen content and dimethylmethylene blue assay for glycosaminoglycan [GAG] content), and biomechanically (compression testing). Collagen content in the CZ was lower than that in the PZ. GAG content in the CZ was higher than that in the PZ. GAG content in the PZ of the posterior portion was significantly higher than that in the anterior and middle portions. Compression strength in the CZ was higher than that in the PZ. The differences in cellular phenotype, vascular penetration, and ECM not only between CZ and PZ but also among the anterior, middle, and posterior portions were clarified in the immature porcine meniscus. This result helps further our understanding of the biological characteristic of the meniscus. © 2014 Orthopaedic Research Society. Published by Wiley Periodicals, Inc. J Orthop Res 32:1602–1611, 2014.

Keywords: meniscus; porcine; extracellular matrix; structure

The meniscus plays an important role in bearing biomechanical stress on the knee joint. It has many functions, including load bearing and transmission, and joint stability, lubrication, and congruity.[1,2] Meniscus tissue contains water (72%), collagens (22%), and glycosaminoglycans (GAGs) (0.8%).[3] The meniscus consists of fibrochondrocytes embedded in an extracellular matrix (ECM) composed of a hydrophilic proteoglycan gel enmeshed in a dense network of type I collagen fibrils. The peripheral vascular portion of the meniscus contains mainly type I collagen, whereas type II collagen occurs in the central avascular portion. Aggrecan is a major proteoglycan in the meniscus. Aggrecan content is higher in the central zone (CZ) than in the peripheral zone (PZ).[4] The composition of the ECM of the meniscus dictates its mechanical properties. Joint loading creates tension within the circumferential fibers of the meniscus and insertional ligament.[5] The proteoglycan constituents of the ECM enable the cartilage to resist compressive loads.[6] The vascularity of the meniscus has considerable clinical significance.[1] These characteristics suggest that knowledge of differences between the CZ and PZ is important.

The meniscus is a C-shaped structure. Not only are zonal (CZ and PZ) structural differences important, but so are differences in anatomic (medial and lateral) and regional (anterior, middle, posterior) location. It was reported that cellular phenotypes, vascular penetration, and ECM differ between CZ and PZ in human and animal models.[2,7] However, the differences among anterior, middle, and posterior portion remain unknown. Proteoglycans predominantly influence the compression loading capacity against compression. A portion of the axial load is transformed into hoop stresses at the meniscal periphery,[1] whereas the radial tie fibers influence the tensile properties of meniscus.[8] However, how the biomechanical property is influenced by the regional differences in GAG and collagen remains unclear.

Since the adult porcine meniscus is an often-used animal model for meniscus repair, its biological characteristics have been reported elsewhere[9]; however, those of the immature porcine meniscus, especially among different locations, is unknown. In the current study, using immature porcine menisci, we investigated the composition of the ECM of the meniscus based on histologic, biochemical, and biomechanical analyses of zonal, regional, and anatomic locations for further understanding of its biological properties.

METHODS

Left and right knees from 20 pigs (age, 6 months) were obtained from a slaughterhouse.

The medial and lateral menisci were removed. First, each meniscus was divided into three regions: anterior, middle, and posterior (Fig. 1). In each portion, the CZ and PZ were compared by histologic, immunohistochemical, biochemical, and biomechanical approaches (Fig. 1). For histologic and immunohistochemical analysis, each piece was cut on the coronal plane (Fig. 1). For scanning electron microscopic (SEM) and biochemical analyses, each piece was first cut on the coronal plane and then divided into two zones (CZ and PZ) (Fig. 1a). A 1-mm-thick sample was cut from the bottom to the top after each piece was cut on the coronal plane (Fig. 1b). The tip of the CZ was trimmed to a 5-mm pillar, while the adherent portion to the joint capsule was trimmed to a 5-mm pillar as the PZ.

Histologic Analysis

First, the specimens were washed with phosphate-buffered saline (PBS) and were fixed in 4% paraformaldehyde (PFA)

Conflict of interest: None.
Grant sponsor: Japan Society for the Promotion of Science of the Ministry of Education, Culture, Sports, and Science; Grant number: 25242055.
Correspondence to: Hiroshi Kuroki (T&F: +81-75-751-3963; E-mail: Kuroki.hiroshi.6s@kyoto-u.ac.jp)

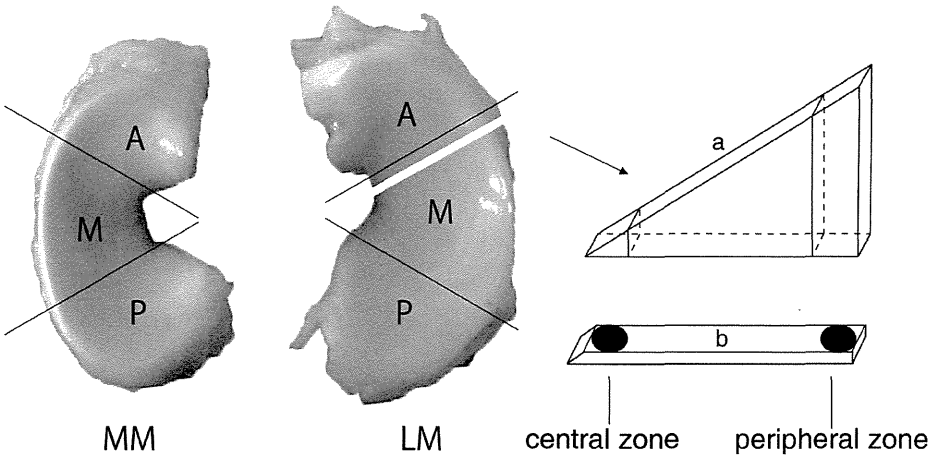

Figure 1. Anatomic, regional, and zonal locations within the right knee joint of a test specimen. The medial meniscus (MM) and lateral meniscus (LM) were divided into three portions: anterior (A), middle (M), and posterior (P). In each portion, the central and peripheral zones were examined. (a) For histologic analysis and immunohistochemical staining, each piece was cut on the coronal plane. For scanning electron microscopic and biochemical analyses, each piece was first cut on the coronal plane and then divided into central and peripheral zones. (b) For the biomechanical analysis, each sample was cut 1 mm thick from bottom to top after each piece was cut on the coronal plane.

at 4°C overnight. Then, the specimens were embedded in paraffin and were cut into 6-μm-thick coronal sections. For all samples, hematoxylin & eosin (H&E), safranin O/fast green, and picrosiriusred staining were performed using standard procedures.

In this study, the diameters of the radial tie fibers[8] were measured using ImageJ software (US National Institutes of Health, Bethesda, MD). The diameters >100 μm were considered large. To quantify the area ratio of the larger radial tie fibers in the PZ, the areas of the large radial tie fibers and a sample of meniscus were measured using ImageJ (US National Institutes of Health) software and the area ratio was calculated.

Immunohistochemical Analysis

Sections were washed with PBS (pH 7.4) and the endogenous peroxidase activity was blocked by 3% hydrogen peroxide for 30 min at room temperature. As primary antibodies, monoclonal mouse anti-pig CD34 antibody (ab81289; Abcam, Cambridge, MA) diluted 1:300 was reacted with the sections overnight at 4°C. Subsequently, the sections were reacted using a Vector Laboratories ABC kit (Vector Laboratories, Burlingame, CA). Staining was visualized using an ImmPACT_DAB kit (Vector Laboratories) with a development time of 45 s. The DAB reaction was stopped by washing with tap water, and counterstaining was subsequently performed with hematoxylin. Sections that were not reacted with the primary antibodies were stained as negative controls. All the control samples tested negative.

To quantify the extent of vascular penetration, the length between the PZ edge of the meniscus and the farthest blood vessel was measured using ImageJ software and then normalized to the total length (from CZ and PZ edge) of the meniscus.[7]

SEM

Each specimen was fixed in a solution containing 2% glutaraldehyde and 4% PFA at 4°C overnight. After washing in 0.1 M phosphate buffer, a second fixation step was performed with 1% osmic acid. The specimens were dehydrated with ethanol, transferred into tert-butyl alcohol, and freeze-dried at −20°C. The dried specimens were mounted on stages, coated with platinum/palladium, and observed using a HITACHI S-4700 electron microscope (Hitachi High Technologies, Tokyo, Japan).[10]

Biochemical Analysis

Hydroxyproline Assay

The CZ and PZ of the samples were digested by 1 ml of 6N HCl at 105°C for 6 h. Chloramine-T was added to the samples for 25 min at room temperature. Ehrlich's reagent was added to each sample, and the solution was reacted by incubating at 65°C for 20 min with shaking. We read the absorbance of each sample at A_{530} nm using a microplate reader (Multiskan; Thermo, Kyoto, Japan).[11] Finally, 13.5% was used as the conversion factor for calculating collagen content.[12]

Dimethylmethylene Blue (DMMB) Assay

Proteoglycan content was estimated by quantifying the amount of sulfated GAGs with a DMMB assay. The CZ and PZ of the samples were digested by 1 ml of papain solution containing 20 mM sodium phosphate buffer (pH, 6.8), 1 m Methylenediaminetetraacetic acid, 2 m Mdithiothreitol, and 300 μg papain at 65° for 6 h. Then, we analyzed GAG content at A_{530} nm using a microplate reader (Multiskan).[13]

The contents were standardized by dividing by the samples' wet weight comparison.

Biomechanical Analysis

For biomechanical analysis, each meniscus portion was cut to be 1-mm thick from the surface of the tibia face (Fig. 1b), as measured by a stereoscopic microscope (Multi viewer system; Keyence, Osaka, Japan). Then unconfined compression was applied from the cutting face of the sample using a mechanical testing instrument (Autograph AG-X; Shimadzu, Kyoto, Japan). Each sample was compressed uniaxially in a

testing chamber filled with PBS at room temperature. A preload of 0.01 N was applied and allowed to equilibrate for 3 min. Then, peak stress was measured when loading was applied at a strain rate of 0.001 mm/s up to 50% strain[14] and maintained for 30 min.

Statistical Analysis

Student's t-test was used for the biochemical comparison between zonal (CZ and PZ) locations and between anatomic locations (lateral and medial menisci), whereas the Tukey post-hoc test (after one-way analysis of variance) was used to

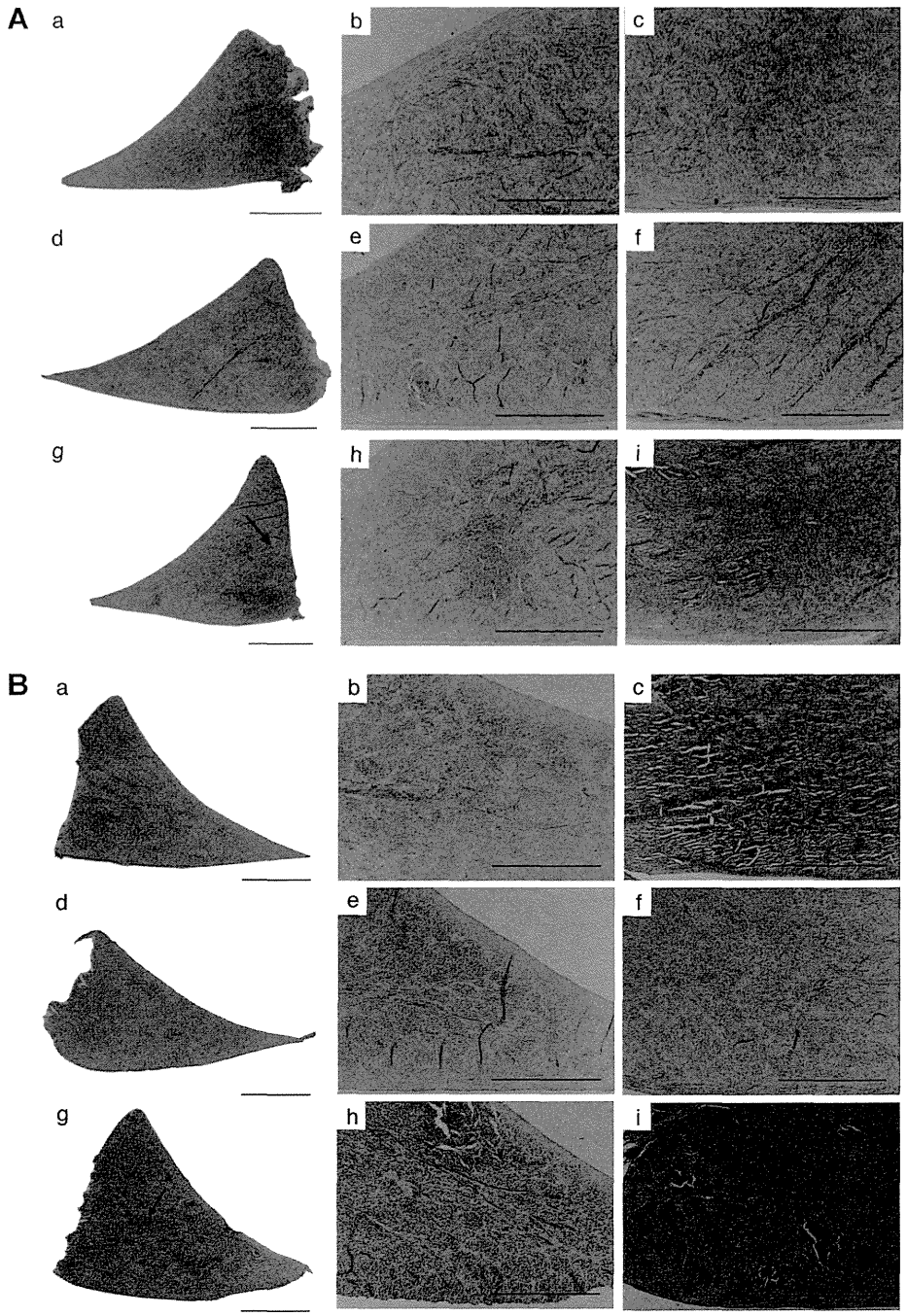

Figure 2. Histologic findings of hematoxylin & eosin staining. (A) Cross sections of the anterior (a), middle (d), and posterior (g) portions of the lateral meniscus. Low power views of the central zone (anterior [b], middle [e], posterior [h]) and peripheral zone (anterior [c], middle [f], posterior [i]). (B) Cross sections of the anterior (a), middle (d), and posterior (g) portions of the medial meniscus. Low power views of the central zone (anterior [b], middle [e], posterior [h]) and peripheral zone (anterior [c], middle [f], posterior [i]). Magnification 40×. Bar = 500 μm. The arrow indicates radial tie fiber.

determine the area ratio of the large radial tie fibers, vascular penetration, and biochemical comparison between regional locations (anterior, middle, and posterior portions). All statistical analyses were performed using SPSS Ver. 20.0.0software (IBM Corporation, Armonk, NY). A p value of <0.05 was considered significant.

RESULTS

Histologic Analysis

H&E staining revealed that the PZ was stained more intensely than the CZ by eosin (Fig. 2A [a, d, g], B [a, d, g]). The radial tie fibers were long in the posterior portion of the meniscus (Fig. 2A [g], B [g] arrow).

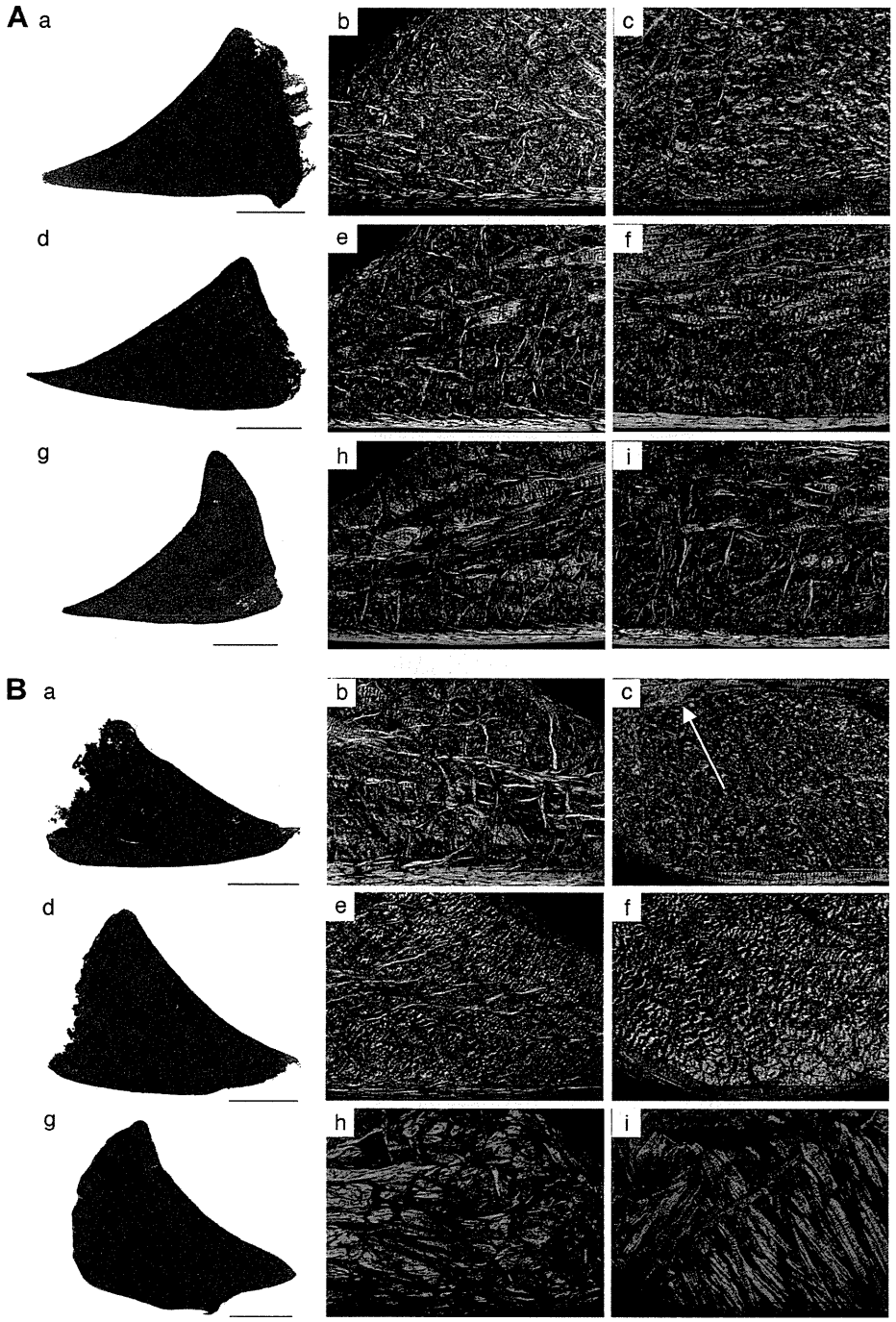

Figure 3. Histologic findings of picrosirius red staining. (A) Cross sections of the anterior (a), middle (d), and posterior (g) portions of the lateral meniscus. Low power views of the central zone (anterior [b], middle [e], posterior [h]) and peripheral zone (anterior [c], middle [f], posterior [i]). (B) Cross sections of the anterior (a), middle (d), and posterior (g) portions of the medial meniscus. Low power views of the central zone (anterior [b], middle [e], posterior [h]) and peripheral zone (anterior [c], middle [f], posterior [i]). Magnification 40×. Bar = 500 μm. The arrow indicates large radial tie fiber.

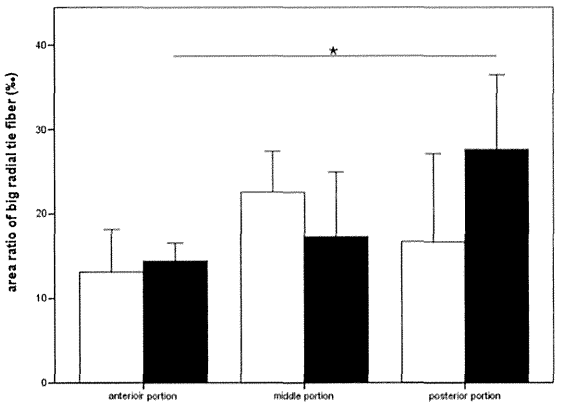

Figure 4. The area ratio of large radial tie fiber. The open box shows the area ratio of large tie fiber of medial of meniscus. The closed box shows the area ratio of large tie fiber of lateral meniscus. $^{*}p < 0.05$. Error bar, ±2 SD.

Angioid tissues were found in the PZ (Fig. 2A [c, f, i], B [c, f, i]), as was reported by Arnoczky and Warren.[15]

Picrosirius red staining demonstrated that collagen fibers were present in the meniscus (Fig. 3). On the surfaces facing the femur and tibia, the collagen fibers were assigned parallel to the surface (Fig. 3A [b–i], B [b–i]). Cross-sections of circumferential fiber bundles and radial tie fibers crossed in the transverse direction were observed. The large radial tie fibers were observed in the PZ (Fig. 3B [c] arrow). The result of area ratio of large radial tie fibers, area ratio in anterior portion was smaller in the posterior portion of lateral meniscus (Fig. 4).

Safranin O staining demonstrated that the CZ was richer in GAGs than in the PZ (Fig. 5). In the CZ, the surfaces facing the femur and tibia did not contain

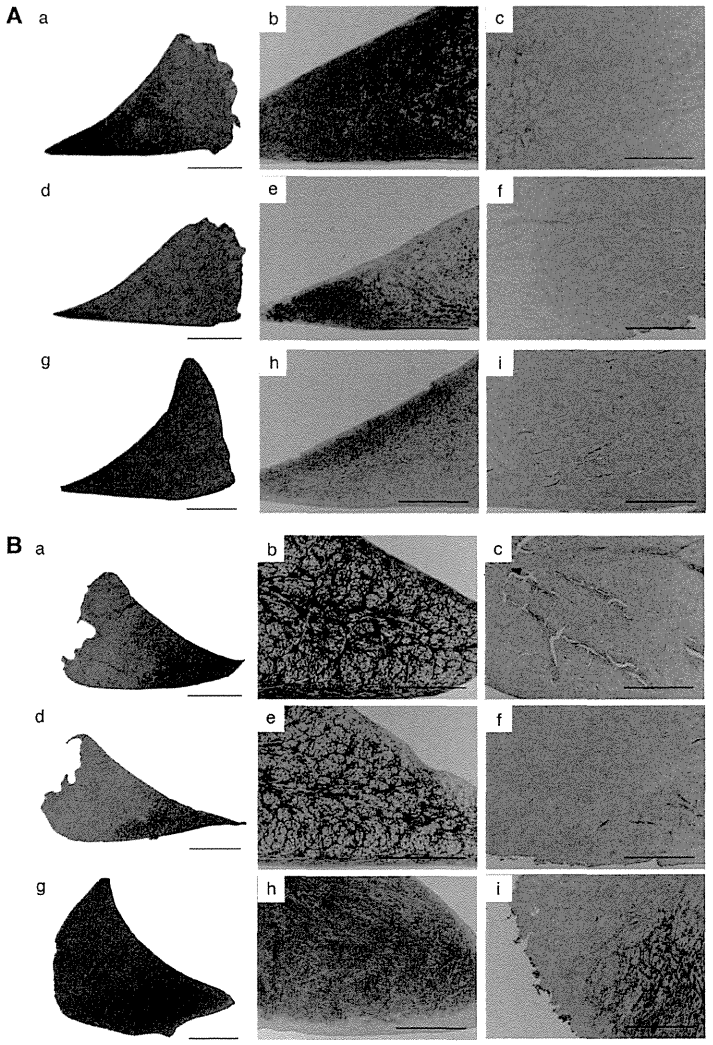

Figure 5. Histologic findings of safranin O/fast green staining. (A) Cross sections of the anterior (a), middle (d), and posterior (g) portions of the lateral meniscus. Low power views of the central zone (anterior [b], middle [e], posterior [h]) and peripheral zone (anterior [c], middle [f], posterior [e]). (B) Cross sections of the anterior (a), middle (d), and posterior (g) portions of the medial meniscus. Higher power views of the central zone (anterior [b], middle [e], posterior [h]) and peripheral zone (anterior [c], middle [f], posterior [i]). Magnification 40×. Bar = 500 μm.

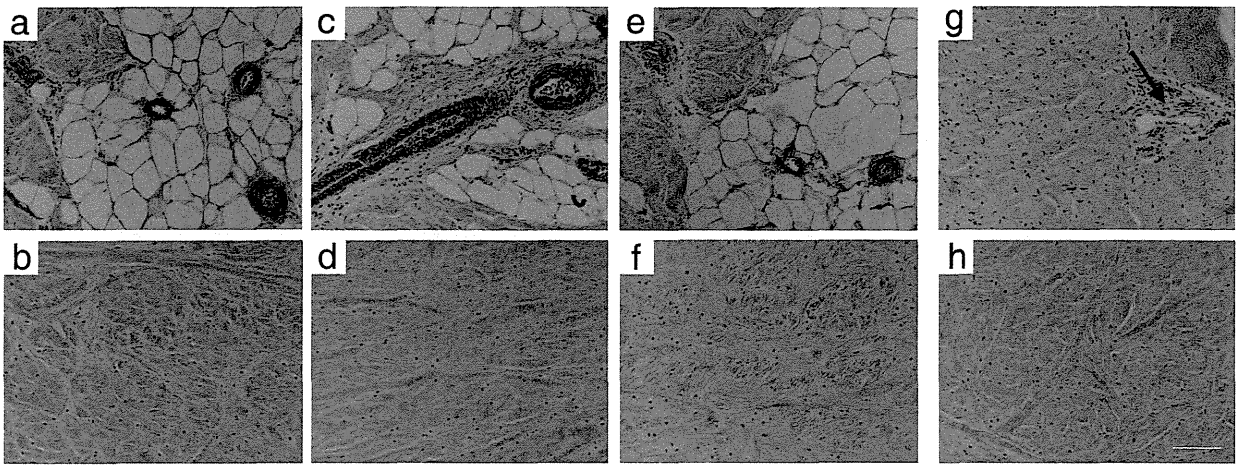

Figure 6. CD34 immunohistochemical staining of medial meniscus high power view of the positive control for the peripheral zone ([PZ] of the anterior [a], middle [c], and posterior [e] portions) and central zone ([CZ] of the anterior [b], middle [d], and posterior [f] portions) of the medial meniscus. Higher power view of the negative control for the PZ (PZ of the anterior portion [g]) and CZ (CZ of the anterior portion [h]) of the anterior portion of the medial meniscus. Arrow, negative control for blood vessels. Magnification 200×. Bar, 100 μm.

GAGs, but the internal portion was rich in them (Fig. 5A [b, e, h], B [b, e, h]).

Histochemical findings showed a clear difference in Safranin O staining between the CZ and PZ and also between the surface and internal portions. The difference in Safranin O staining was not so clear between the lateral and medial menisci or between the anterior, middle, and posterior portions. On picrosirius red staining, the differences among zonal locations and among regional locations were unclear.

Immunohistochemical Analysis

Immunohistochemistry revealed the blood vessel distribution. The vascular penetration was primarily noted in the PZ but invaded the PZ of the synovial tissue. After hematoxylin counterstaining, round fibrochondrocytes and spindly fibroblast-like cells were visible in the CZ and PZ, respectively (Fig. 6). The percentage of vascular penetration was 10–30%, and that of the posterior portion of the medial meniscus was the greatest ($p < 0.05$). In the lateral meniscus, the vascular penetration in the middle portion was higher than that in the others ($p < 0.05$). In addition, the differences between the medial and lateral menisci in the anterior, middle, and posterior portions were significant ($p < 0.05$; Fig. 7).

SEM

It was observed that the orientation of the collagen fibers was different between the surface and internal portions (Fig. 3). The collagen fibers facing the femur and tibia formed layers parallel to the surface (Figs. 8 and 9 [a, b, c, g, h, i]); the density of collagen fibers facing the femoral side (Figs. 8 and 9 [a, b, c]) were lower than that of those facing the tibial side (Figs. 8 and 9 [g, h, i]). There was no significant difference between the surface of the CZ (Fig. 8 [a, b, c, g, h, i]) and that of the PZ (Fig. 9 [a, b, c, g, h, i]). The density of collagen fibers in the internal portion of the CZ (Fig. 8 [d, e, f]) was similar to that in the surface portion. However, the density of collagen fibers in the internal portion of the PZ (Fig. 9 [d, e, f]) was quite different from that in the surface portion. The differences among the anterior, middle and posterior portions were unclear.

Biochemical Analysis

The hydroxyproline assay demonstrated that collagen content in the PZ was higher than that in the CZ

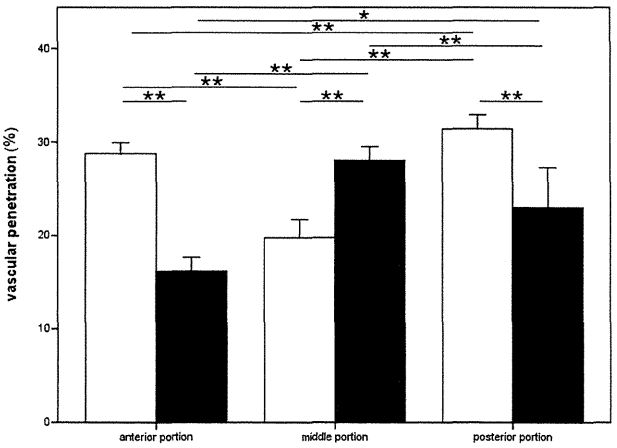

Figure 7. Vascular penetration of meniscus. The open box shows the vascular penetration of medial portion, whereas the closed box shows the vascular penetration of lateral meniscus. $^{*}p < 0.05$, $^{**}p < 0.01$. Error bar = ±2 SD.

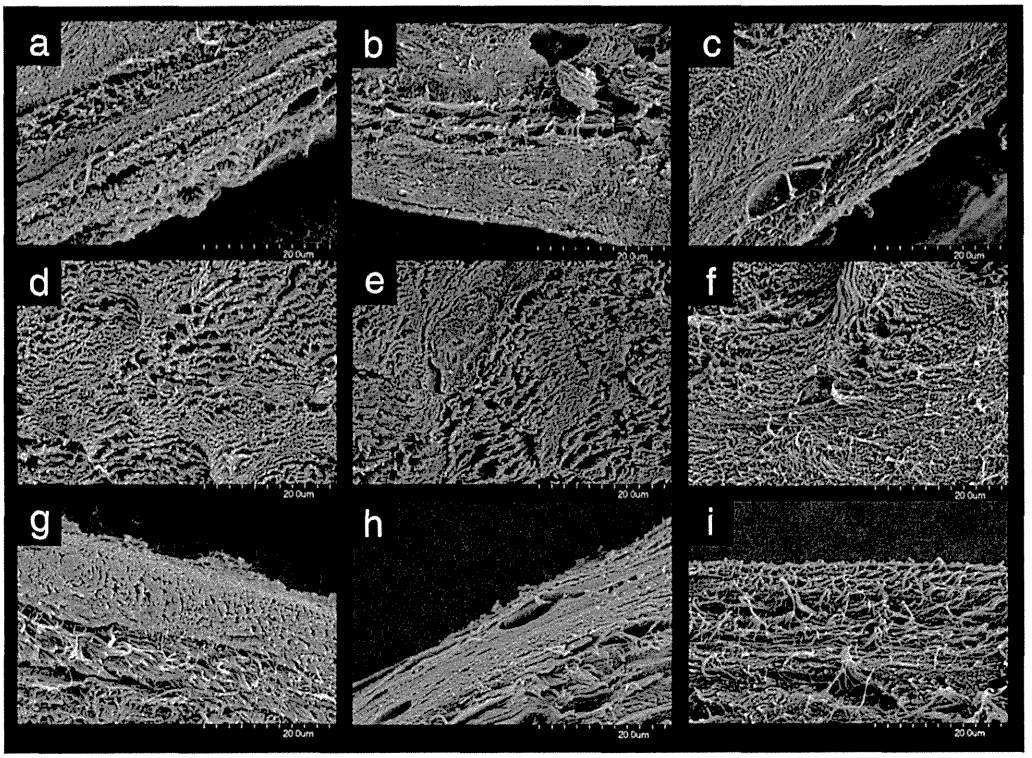

Figure 8. Scanning electron microscopic image of the central zone (CZ) of lateral meniscus. the CZ in the anterior (surface of femoral side [a], inner layer [d], surface of tibial side [g]), middle (surface of femoral side [b], inner layer [e], surface of tibial side h]) and posterior (surface of femoral side [c], inner layer [f], surface of tibial side [i]) portions. Magnification 1,500×. Bar = 20 μm.

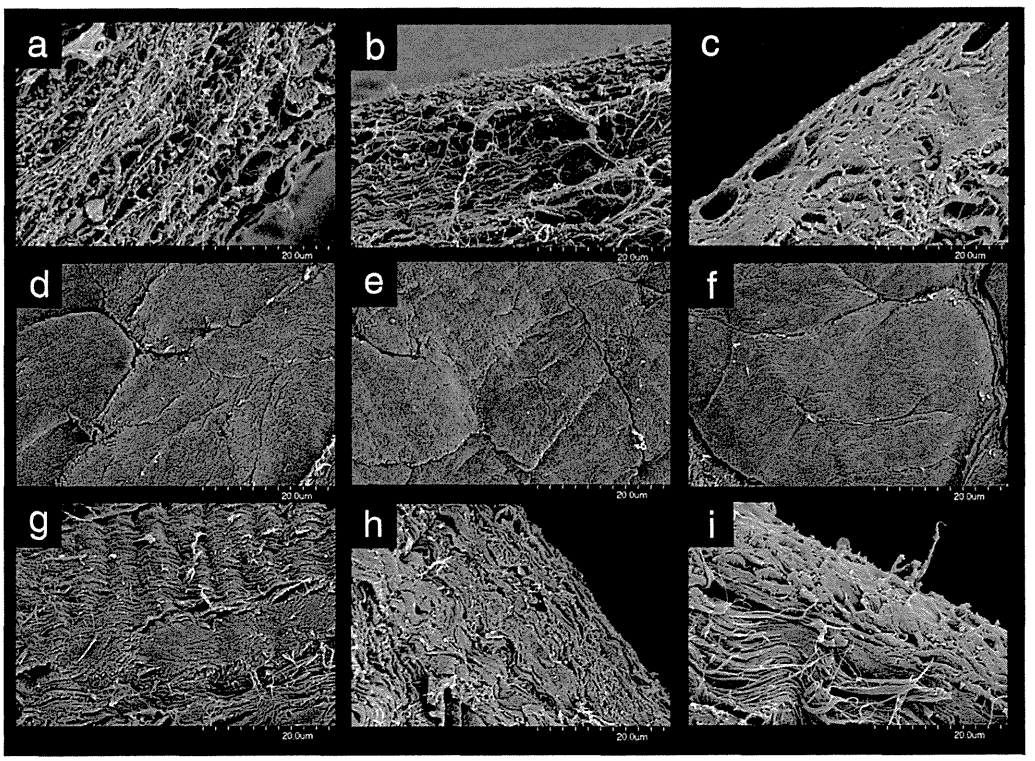

Figure 9. Scanning electron microscopy image of the peripheral zone (PZ) of the lateral meniscus. The PZ in the anterior (surface of the femoral side [a], inner layer [d], surface of the tibial side [g]), middle (surface of the femoral side [b], inner layer [e], surface of the tibial side [h]), and posterior (surface of the femoral side [c], inner layer [f], surface of the tibial side [i]) portions. Magnification 1,500×. Bar, 20 μm.

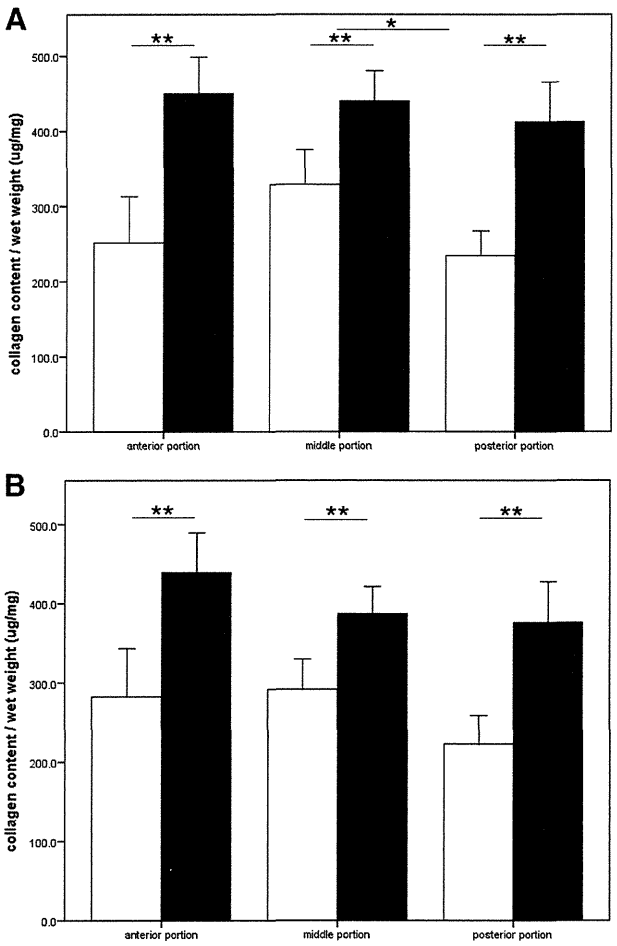

Figure 10. Collagen content of the lateral (A) and medial (B) menisci. The open box is collagen content of the central zone, while the closed box is collagen content of the peripheral zone in each region. $^{*}p < 0.05$, $^{**}p < 0.01$. Error bar, ±2 SD.

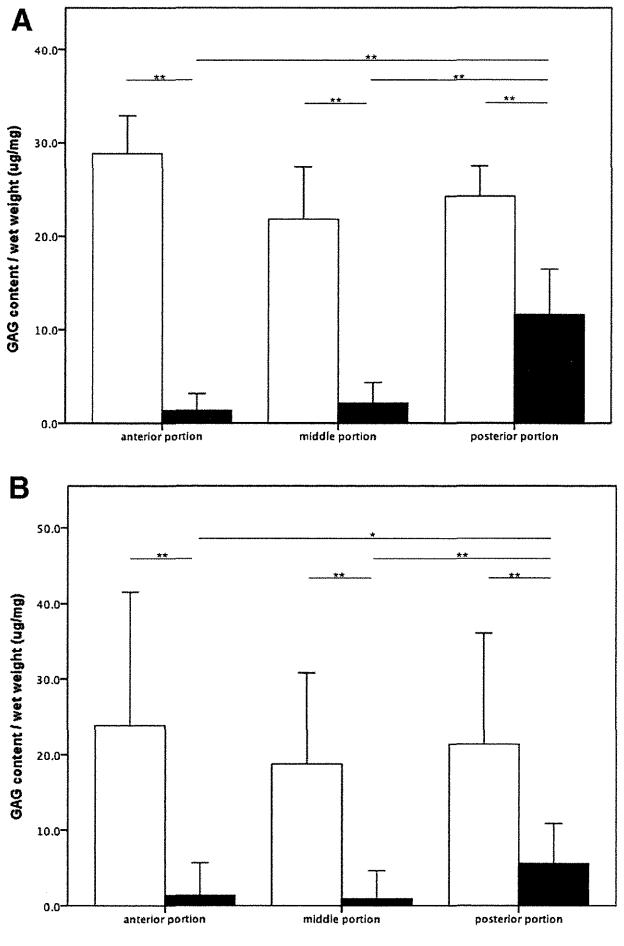

Figure 11. Glycosaminoglycan (GAG) content of the lateral (A) and medial (B) menisci. The open box is GAG content of the central zone, while the closed box is GAG content of the peripheral zone in each region. $^{*}p < 0.05$, $^{**}p < 0.01$. Error bar, ±2 SD.

(Fig. 10). The large radial tie fibers found in picrosirius red stain (Fig. 3 [c]) may reflect this difference. In the CZ of the lateral meniscus, the collagen content of the middle portion was significantly higher than that in the posterior portion (Fig. 10A and B).

The DMMB assay showed that GAG content in the CZ was higher than that in the PZ (Fig. 7A and B). GAG content in the PZ of the posterior portion was significantly higher than that in the anterior ($p < 0.01$ in the lateral meniscus, $p < 0.05$ in the medical meniscus) and middle ($p < 0.01$ in both menisci) portions (Fig. 11A and B). In addition, GAG content in the PZ of the posterior portion of the lateral meniscus was significantly higher than that of the medial meniscus ($p < 0.05$).

Biomechanical Analysis

Results of compression testing showed that the CZ had significantly higher peak stress strength than the PZ ($p < 0.05$, Fig. 12A and B). In the medial meniscus, the anterior portion was significantly higher than the posterior portion ($p < 0.05$, Fig. 12B).

DISCUSSION

The main cellular phenotype of the inner and middle part of human meniscus has been termed the round fibrochondrocytes, however the outer portion of the meniscus is primarily populated by spindly fibroblast-like cells.[2] In meniscus cellular phenotype, we found the similar finding in immature porcine. With regards to vascular penetration of this study, CD34 expression was observed in 10–30% of the PZ of the menisci. This result is consistent with the vascular penetration in human reported by Arnoczky and Warren.[15]

Fibrocartilaginous tissues such as the knee meniscus that are subjected to both tension and compression contain relatively large amounts of collagen and proteoglycans.[16] It is important to understand zonal differences between each region. The current and previous studies have shown that collagen content in